Electronic Supplementary Material (ESI) for Soft Matter.

Supplementary Information

Responses of Vesicle Shape to Dense Inner Active Matter

Myeonggon Park,[a, b] Kisung Lee,[b] and Steve Granick,[*a, b, c]

[a]Department of Physics, Ulsan National Institute of Science and Technology (UNIST), Ulsan 44919, South Korea

[b]Center for Soft and Living Matter, Institute for Basic Science (IBS), Ulsan 44919, South Korea

[c]Department of Chemistry, Ulsan National Institute of Science and Technology (UNIST), Ulsan 44919, South Korea

Captions of Supplementary Videos

Each video lasts 10 s and is played in real time.

Supplementary Video 1: This movie, accompanying Fig. 2(a), shows that a rigid GUV maintains spherical shape (circular shape in these microscope images) despite vigorous motion by confined dense bacteria.

Supplementary Video 2: This movie, accompanying Fig. 2(b), shows that a softer GUV can be deformed significantly by collective swimming of confined dense bacteria. This GUV repeatedly stretches, then relaxes to a circular shape.

Supplementary Video 3: This movie, accompanying Fig. 2(c), shows that a yet softer GUV also displays transient protrusions. After the impinging bacteria reorient, membrane elasticity causes circular shape to be recovered.

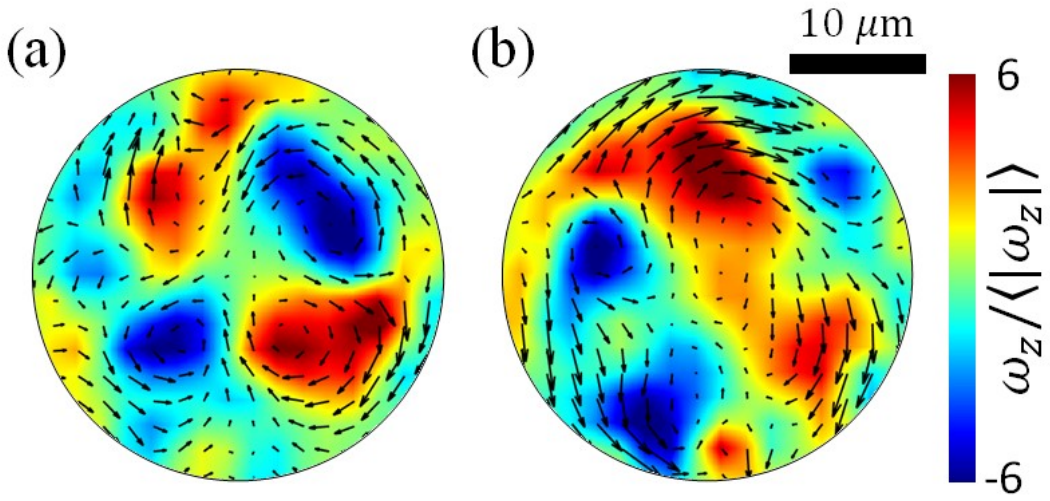

Supplementary Figure 1 Collective dynamic patterns of bacteria in GUVs. Various dynamic patterns appear, intermediate between the vortex and a dipolar flows in Fig. 3(a). (a) Quadrupolar flow where two clockwise vortices and two anticlockwise vortices coexist. (b) Example of a dynamic pattern in which vortices are distributed randomly. Chaotic-looking images such as panel b are most common in our experiments.

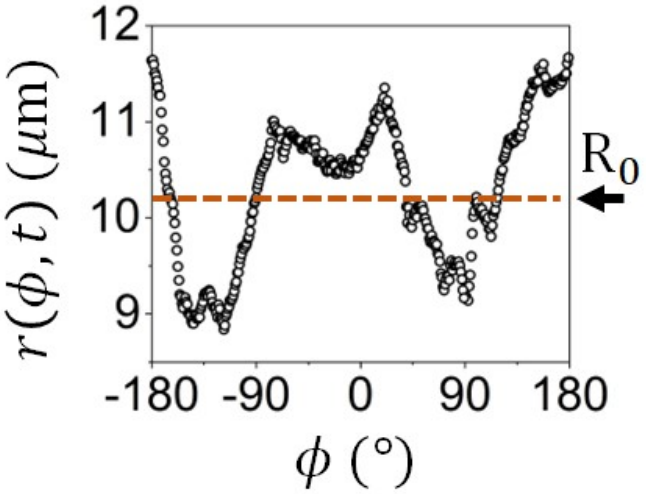

Supplementary Figure 2. Representative contour of a low-tension GUV. Here, $r(\phi,t)$ is extracted from the raw image in Fig. 5(a). $R_0 = < r(\phi,t) >$ is the vesicle radius averaged over ϕ and t. $R_0 = 10.2\ \mu m$

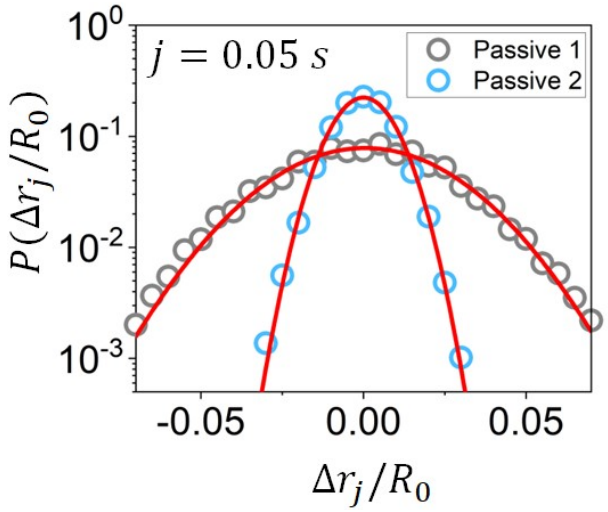

Supplementary Figure 3. Probability distribution function (PDF) of normalized radial fluctuations $^{\Delta r_j/R_0}$ of two passive GUVs, where $^{\Delta r_j = r(\phi,t+j) - r(\phi,t)}$ at j (lag time) of 0.05 s. Contrary to the active GUVs in Fig. 5(b) and (c), the distributions of these GUVs are fitted well by the Gaussian function, as indicated by red lines.

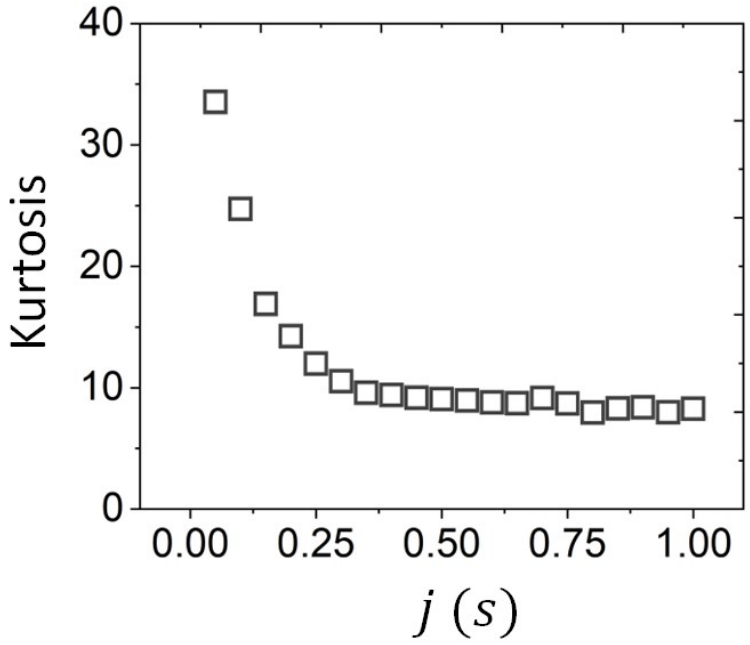

Supplementary Figure 4. Kurtosis of PDF of a low-tension GUV containing encapsulated bacteria, plotted against the interval time , where is a lag time. Kurtosis is the degree of tailedness of PDF; for a Gaussian function, kurtosis = 3 But here, kurtosis = 33 at the smallest lag time, which means it is most nonequilibrium on shortest time scales, then it monotonically decreases to kurtosis = 6, which signifies nonequilibrium dynamics regardless of .

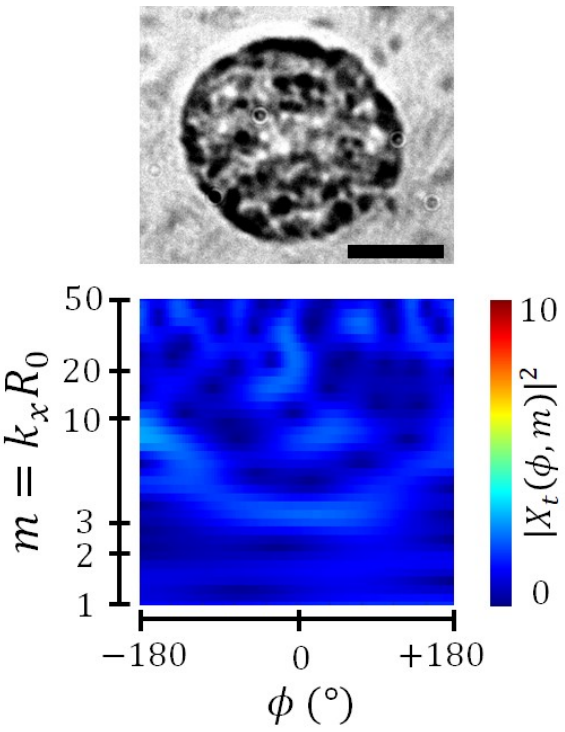

Supplementary Figure 5. An image of a circular GUV and the associated intensity ($|X_t(\phi,m)|^2$) from continuous wavelet transform (CWT) analysis using the Morse wavelet, whose magnitudes are identified on the color map scale on the right. The CWT intensity is homogeneously low, in contrast to Fig. 6(a) and (b), because $r(\phi,t)$ of this membrane is almost flat. Scale bar in the top image is $10\ \mu m$.

Fitting a $\langle|\hbar(k_x,t)|^2\rangle$ (height fluctuation) spectrum

The contour edge is projected to a Fourier series with 50 modes by

$$r(\phi,t) = R(t)\left(1 + \sum_{m=1}^{50} a_m \cos m\phi + b_m \cos m\phi\right), \quad (1)$$

where $R(t)$ is the radius of GUV at time t and m is the mode number. Then the height fluctuations are defined by

$$\langle|\hbar(k_x,t)|^2\rangle = \frac{\pi R_0^3}{2}\left(\langle|c_m|^2\rangle - \langle|c_m|\rangle^2\right), \quad (2)$$

where $R_0 = \langle r(\phi,t)\rangle$ is the time-averaged radius of GUV, $k_x = m/R_0$ is the wave vector, and the Fourier coefficients are $|c_m| = \left(a_m^2 + b_m^2\right)^{1/2}$.

According to Supplementary Video 2 and the CWT analysis in Fig. 6(a) and (b), the active fluctuations are primarily induced by collective bacteria motion. Therefore, we extracted the membrane tension (λ) and bending modulus (κ), using the Helfrich Hamiltonian to fit $\langle|\hbar(k_x,t)|^2\rangle$ of high mode number. Helfrich in Fig. 6(c) is fitted by $\lambda = 3\ pN/\mu m$, $\kappa = 30\ k_BT$, and $R_0 = 10\ \mu m$, which were also used for the active membrane.

The Takatori-Sahu model, developed to explain the active fluctuations by a contact force of individual bacteria, predicts the analytic function for $\langle|\hbar(k)|^2\rangle$:

$$\langle|\hbar(k)|^2\rangle = \frac{k_BT}{\kappa k^4 + \lambda k^2} + \frac{N_p\tau_R}{\tau_T + \tau_R}\left(\frac{a^2\bar{p}/R_0}{\kappa k^4 + \lambda k^2}\right)^2 e^{-a^2k^2}, \quad (3)$$

where λ is the tension, κ is the bending modulus, a is the size of a swimming body assuming a spherical shape, τ_R is the bacterial reorientation time, τ_T is the time it takes the bacteria to travel one side of vesicle to another, N_p is the number of bacteria confined to a GUV, and $\bar{p}$ is the maximum pressure applied to the membrane by a bacterium.

To compare Eq. (3) with experiments, the height fluctuations of the nearly planar membrane are averaged over k_y modes. In practice, the average is done numerically by

$$\langle|\hbar(k_x,t)|^2\rangle = \frac{2}{L}\sum_{n=0}^{M}\langle|\hbar(k=(k_x,2\pi n/L),t)|^2\rangle, \quad (4)$$

In fits to the original Takatori-Sahu (TS) model to fit our experiment in Fig. 6(c), we use the parameters $N_p = 100$ and $a = 0.25\ \mu m$,the half width of a bacterium. In the dense bacteria system, we specify parameters in the equation by reasoning as follows. First, $N_p = 1$ because dense bacteria move collectively like a single body. From our experiment, $\tau_R \approx 0.25\ s$ (see

Supplementary Fig. 6) and $\tau_T \approx 2R_0/U_0 \approx 2\ s$ is the time for a swimming group to traverse the vesicle diameter $2R_0 \approx 20\ \mu m$, moving at speed $U_0 \approx 10\ \mu m/s$ in a dense environment.

The size of swimming group, which gives a contact force to the GUV, assumes a spherical shape. Therefore, we defined $a \approx 3\mu m$ based on the fluctuating contour of GUVs (see Supplementary Fig. 7). It is much larger than the half-width of a bacterium $(0.25\ \mu m)$.

We approximated the pressure exerted on the membrane by the group of bacteria as $\bar{p} \approx \lambda/a$. In fact, because the flocking cluster can stretch the membrane, this may reduce the actual contact pressure slightly.

Experimental height fluctuations in Fig. 6(c) are fitted with different parameters:

Top panel: $\kappa = 30\ k_BT$, $\lambda = 3\ pN/\mu m$, and $R_0 = 10\ \mu m$.

Middle panel: $\kappa = 40\ k_BT$, $\lambda = 1.5\ pN/\mu m$, and $R_0 = 11\ \mu m$.

Bottom panel: $\kappa = 25\ k_BT$, $\lambda = 0.7\ pN/\mu m$, and $R_0 = 9\ \mu m$.

N_p, a, τ_R, τ_T were the same with discussed values above.

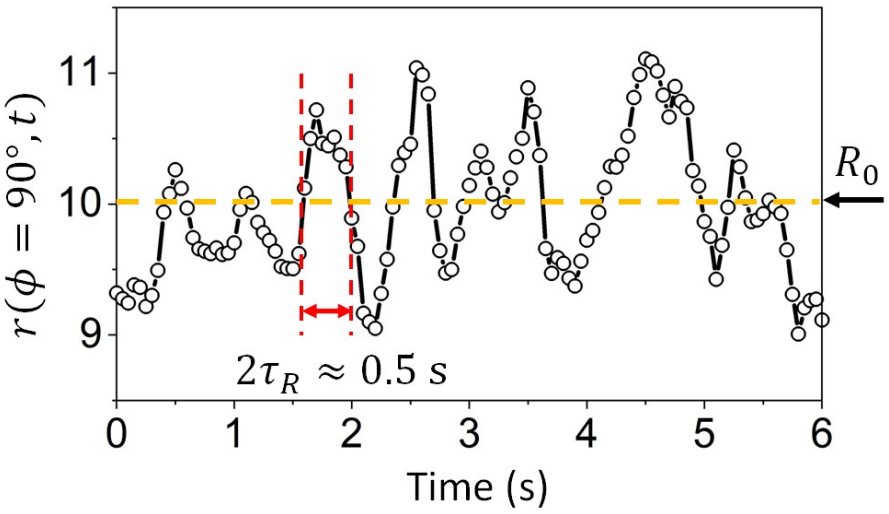

Supplementary Figure 6 The radial position of contour $r(\phi = 90°,t)$ fluctuates in time owing to bacteria activity. Noticing that the period of stretch and relaxation is $\approx 0.5\ s$, we set $\tau_R \approx 0.25\ s$ in the comparison to Eq. (3).

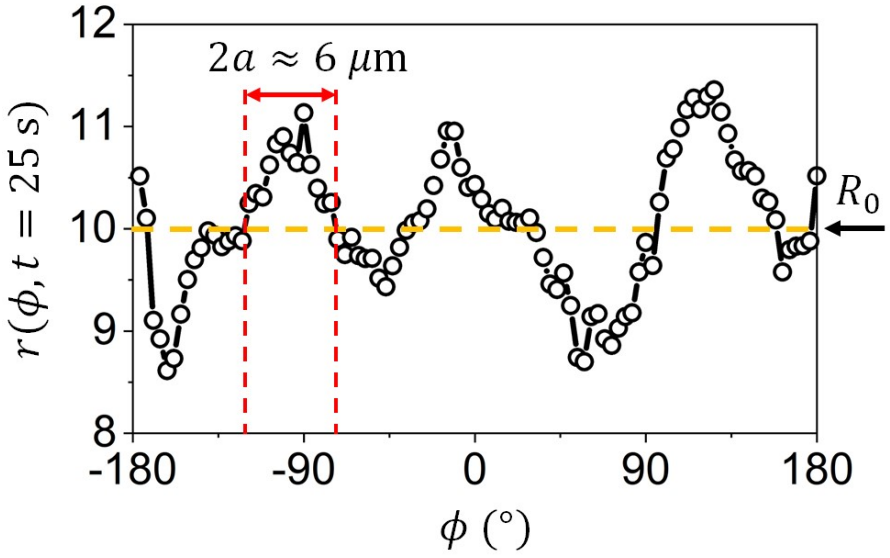

Supplementary Figure 7 The radial position of contour $r(\phi,t = 25\ s)$ fluctuates in time owing to bacteria activity. Noticing the periodic bumps with widths $\approx 6\ \mu m$, we define $a \approx 3\ \mu m$ as radius of the swimming group, which is spherical for comparison to Eq. (3).